Materials Science in Semiconductor Processing 75 (2018) 183–192

Contents lists available at ScienceDirect

Materials Science in Semiconductor Processing

journal homepage: www.elsevier.com/locate/mssp

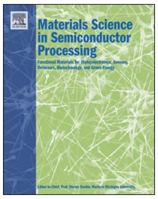

Heterojuncted non-metal binary composites silicon carbide/g-C_3N_4 with enhanced photocatalytic performance

Fei Chang[a,*], Jiaojiao Zheng[a], Xiaofang Wang[a], Quan Xu[a], Baoqing Deng[a], Xuefeng Hu[b,*], Xiaoqi Liu[c]

[a] School of Environment and Architecture, University of Shanghai for Science and Technology, Shanghai 200093, PR China
[b] Key Laboratory of Coastal Environmental Processes and Ecological Remediation, Yantai Institute of Coastal Zone Research, Chinese Academy of Sciences, Yantai, Shandong 264003, PR China
[c] Institute of Tianjin Seawater Desalination and Multipurpose Utilization, State Oceanic Administration, Tianjin 300192, PR China

ARTICLE INFO

Keywords:
SiC
g-C_3N_4
Heterojunction
Photocatalysis
Active radicals
Mechanism

ABSTRACT

Novel visible-light-driven silicon carbide (SiC)/g-C_3N_4 heterojuncted composites were successfully prepared via a facile ultrasonic dispersion and calcination method, and afterwards characterized by a couple of technologies including XRD, SEM, TEM, FT-IR, XPS, UV–vis DRS, PL spectra, and N_2 adsorption-desorption. It was found that SiC nanoparticles were uniformly deposited over the surface of g-C_3N_4 to create heterojunction domains along phase interface boundary, favoring charge carriers transfer and separation across the straddling band alignments. Besides, the visible-light absorption capability of samples was enhanced by the incorporation of SiC. These physiochemical merits ensured the improved photocatalytic performance of heterojuncted composites over the degradation of dyes rhodamine B (RhB) and methyl orange (MO) in comparison to each single component SiC or g-C_3N_4. Upon an identical condition, the sample SN8 exhibited the highest photocatalytic ability among all tested samples. According to active species trapping measurements, $\cdot OH$ and $\cdot O_2^-$ were deemed as major radicals and eventually a possible photocatalysis mechanism was speculated.

1. Introduction

Wastewaters containing synthetic dyes and pigments such as rhodamine B, methyl orange, and indigo carmine discharged from manufactories inadequately addressed cause serious environmental pollution, directly affecting human health and well-being [1,2]. On account of their complicated aromatic structure and thermos-stability, most dyes are hardly decomposed by conventional physical or biochemical treatments. Instead, the photocatalytic technology, a sustainable and green route, is able to dispose of these contaminants through an oxidative degradation process. Therefore, burgeoning highly efficient visible-light-driven semiconductor-based photocatalysts becomes a matter of great urgency in the field of eliminating environmental contaminations and even converting solar energy [3,4]. A single-phased photocatalyst suffers from the fast combination of photoinduced electron-hole pairs plus relatively low photocatalytic capability, while the construction of a binary system with suitable band structures seems to be an effective manner to conquer this limitation because the charge carries are promoted to transfer in opposite directions through a smooth phase interfaces, so as to reduce the recombination efficiently and further promoting the photocatalytic performance [5,6]. In addition, incorporating a narrow band-gap component also conduce to the visible-light harvesting and then heighten the visible-light response of hybrid composites.

So far, the polymeric graphite-like carbon nitride (g-C_3N_4), recognized as a favorite metal-free polymeric material, has garnered particular attention in fields of water splitting for hydrogen evolving [7] and pollutant decomposition under visible light irradiation [8,9] by virtue of its appealing electronic properties as well as high thermal and chemical stability [10,11]. However, g-C_3N_4 served as a photocatalyst alone is real pinned down to its small specific surface area and severe recombination of photogenerated charge carriers [11,12]. A variety of attempts have been employed to modify g-C_3N_4, such as elements deposition [13,14], textural turning [12,15] and building a g-C_3N_4-based heterojunction with Bi_2WO_6 [16], $HSbO_3$ [17], BiOCl [18], WO_3 [19], Ag_3PO_4 [8], $CuCr_2O_4$ [20], and YVO_4 [21] etc. Specifically, Liu et al. successfully synthesized chlorine-intercalated g-C3N4 through a soaking-copyrolysis method [22]. Huang et al. reported the synthesis of porous g-C3N4 thin nanosheets by means of a template-free thiourea-assisted hydrothermal protocol [23]. Tian et al. prepared a 3D

---

* Corresponding authors.
E-mail addresses: feichang@usst.edu.cn (F. Chang), xfhu@yic.ac.cn (X. Liu).

https://doi.org/10.1016/j.mssp.2017.11.043
Received 12 September 2017; Received in revised form 22 November 2017; Accepted 29 November 2017
1369-8001/

mesoporous ultrathin g-C3N4 through a precursor-recrystallization process [24]. These modified g-C_3N_4 samples showed the significant enhancement of photo-absorption and photocatalytic degradation capabilities. Mousavi et al. constructed a series of multicomponent g-C3N4/Fe_3O_4/Ag_3PO_4/AgCl composites by a facile ultrasonic-irradiation method [25] and g-C3N4/Fe_3O_4/Ag_3PO_4/Co_3O_4 composites via ultrasonic and calcination methods as well [26]. Akhundi et al. prepared various quaternary g-C3N4/Fe_3O_4/AgI/Bi_2S_3 catalysts by adding different amount of Bi_2S_3 using a facile refluxing method [27] and further quaternary g-C3N4/Fe_3O_4/Ag/Ag_2SO_3 composites by anchoring the Ag/Ag_2SO_3 system on surface of g-C3N4/Fe_3O_4 in the same manner [28]. Among numerous modification strategies, the semiconductor coupling is regarded as an effective and efficacious manner to combine the advantages of intrinsic structural features from each component phase and possibly bring about a synergistic effect after hybridization [29–32].

SiC is another typical non-metallic semiconductor with an appropriate band gap of 2.3–3.3 eV [33], a more negative conduction band potential, a sufficient thermal and chemical stability, and a high mechanical strength [34], which render it extensively applied in power electronics, radio frequency devices, grinding materials [33], and to be a promising catalyst candidate under visible-light irradiation. Moreover, its high charge-carrier mobility can shuttle the photogenerated carriers swiftly before recombination from the bulk to the surface [33]. Unfortunately, the pure SiC actually exhibits a very weak photocatalytic activity, if any, from the visible to ultraviolet light as a result of the acute recombination of photogenerated charge carriers [35] and low optical response [36]. Gao et al. clearly stated the inferior photocatalytic capability of commercial α-SiC powder for water splitting under visible light in view of its small surface areas [37]. Considering the potential applications, the photocatalytic performance of SiC is generally heightened by modified its microstructure and morphology such as the morphology control [38], noble metal deposition [39], and semiconductor coupling [35,40]. Wang et al. separately deposited Pt and IrO_2 on micro-SiC surface, attaining a synergetic effect to suppressed the carriers recombination and hereby enhancing the photocatalytic activity [41]. Zou et al. attempted to decompose toluene by porous TiO_2/SiC nanocomposite films [42]. Wang et al. found that the average H_2 evolution rate increased to 4572 μl g^{-1} h^{-1} as soon as the Pt/SiC nanowire hybrid was present [43]. If g-C_3N_4 is adopted as another ingredient to construct a composite, the well-matched band positions between SiC and g-C_3N_4 ought to kinetically facilitate the carriers transfer and separation, thereupon giving rise to the enhanced photocatalytic degradation outcome.

In this work, we attempted to construct SiC/g-C_3N_4 heterojuncted hybrids via a simple ultrasonic dispersion and calcination route. The as-synthesized samples were systematically characterized by XRD, SEM, TEM, FT-IR, XPS, UV–vis DRS, PL spectra, and N_2 adsorption-desorption techniques. It was confirmed that SiC, a component with satisfactory visible-light absorption ability, was successfully deposited on the surface of g-C_3N_4 as irregular nanoparticles. What boosted phtocatalytic efficiency over dyes degradation the produced composites take on comparing to bare SiC or g-C_3N_4 mainly owned to the favorable structural and electronic features of composites, such as strengthened light harvesting, uniform generation of heterojunction domains, and efficient separation of charge carriers along well-matched band structures. A possible photocatalysis mechanism was finally speculated based upon active radicals entrapping experiments.

2. Experiment

2.1. Materials and reagents

All chemicals of the reagent grade were utilized as received without further purifications and deionized water purified by a millipore system was used for syntheses and photocatalytic processes. Melamine, MO, disodium ethylenediaminetetraacetate dehydrate (EDTA-2Na), terephthalic acid (TA), sodium hydroxide (NaOH), L-ascorbic acid, isopropanol alcohol (IPA), and absolute ethanol were all purchased from Sinopharm Chemical Reagent Co., Ltd. (Shanghai, China). Both SiC and RhB were provided by Shanghai Mstar Technology Ltd. and Shanghai SSS Reagent Co., Ltd. (Shanghai, China), respectively.

2.2. Samples fabrication

The pure g-C_3N_4 was produced by heating treated melamine in a semi-closed system. In a typical protocol, a desired amount of melamine with 50 mL absolute ethanol was ultrasonicated for 0.5 h and subsequently stirred for 2 h. A solid powder was segregated by filtration, dried at 60 °C for 12 h, carefully ground, charged in a semi-closed ceramic crucible, calcined in a furnace at 550 °C for 1 h with a heating rate of 10 °C min^{-1}, and finally collected as a pale-yellow powder.

As for the synthesis of SiC/g-C_3N_4 hybrid composites, a similar procedure was conducted to the above preparation except the addition of desired amount of SiC during agitation. Based upon the yield of pure g-C_3N_4 as described, changeable amounts of SiC were added and produced samples were labeled as SN0, SN1, SN5, SN8, SN20, and SN50, corresponding to the expected mass ratios of 0 (pure g-C_3N_4), 1%, 5%, 8%, 20%, and 50%, respectively. The N-TiO_2 was also constructed for comparison via a sol-gel method as previously reported [44].

2.3. Characterization

The crystal structure and surface chemical composition were analyzed by a Bruker D8 Advance X-ray diffractometer (XRD, Cu K α radiation source $\lambda = 1.05406$ Å) at 40 kV and 40 mA with a continuous scanning pattern in the range of 5–80° and X-ray photoelectron spectroscopy (XPS, Thermo Scientific ESCALAB 250Xi, exciting source Al K α radiation, $h\nu = 1486.8$ eV). The C1s band was set on 284.6 eV as a reference to calibrate other binding energies. A scanning electron microscopy (SEM, QUANTA F250) and transmission electron microscopy (TEM, Tecnai G2 F20) were employed to measure the morphological and microstructural properties. The UV–vis diffuse reflectance spectra (UV–vis DRS) were analyzed on a spectrophotometer (Shimadzu UV2600, Japan) ranging from 200 to 800 nm for detecting optical features of samples and the $BaSO_4$ was used as a reflectance standard. Fourier-transform infrared (FT-IR) spectra were taken on a Bruker V-70 Fourier transform-infrared spectrophotometer in the frequency range of 500–4000 cm^{-1}. Photoluminescence (PL) spectra were recorded on an Edinburge FLSP920 fluorescence spectrometer. N_2 adsorption-desorption isotherms were evaluated on a Micromeritics ASAP2020HD88 system at 77 K and the pore size distribution was calculated by the Barrett-Joyner-Halenda (BJH) method. All samples were degassed at 120 °C for 4 h prior to measurements.

2.4. Photocatalytic activity evaluations

The photocatalytic behavior of as-prepared samples was checked over the degradation of dye RhB and MO in a photocatalytic reactor. A 300 W Xenon lamp (CEL-HXF300, AuLight, Beijing) was served as a visible light source with a 420–780 nm cut-off filter fixed to assure the presence of only visible light. The reactor stayed in a water channel with a continuous circulation of cold water to maintain a constant temperature and the light source was 20 cm away from the surface of aqueous suspension. The photocatalyst (20 mg) was immersed in an aqueous solution of RhB (20 mg L^{-1}, 80 mL) or MO (5 mg L^{-1}, 80 mL) under a continuous stir. Prior to the visible-light illumination, the suspension was strongly magnetically stirred in dark for 1 h to reach an adsorption-desorption balance between organic molecules and catalysts surface. During irradiation, 3 mL aliquot was taken from the suspension at every 30 min intervals and separated by centrifugation twice. The residue concentrations of RhB and MO were estimated on a UV–vis